

Efficient Data Averaging for Spin Noise Spectroscopy in Semiconductors

Georg M. Müller,^{1, a)} Michael Römer,¹ Jens Hübner,¹ and Michael Oestreich¹

Institut für Festkörperphysik, Leibniz Universität Hannover, Appelstraße 2, D-30167 Hannover, Germany

(Dated: 13 August 2018)

Spin noise spectroscopy (SNS) is the perfect tool to investigate electron spin dynamics in semiconductors at thermal equilibrium. We simulate SNS measurements which utilize real-time fast Fourier transformation instead of an ordinary spectrum analyzer and show that ultrafast digitizers with low resolution enable surprisingly sensitive, high bandwidth SNS in the presence of strong optical background shot noise. The simulations reveal that optimized input load at the digitizer is crucial for efficient spin noise detection while the resolution of the digitizer, i.e., the bit depth, influences the sensitivity rather weakly.

Spin noise spectroscopy (SNS) has emerged into a powerful tool to study the spin dynamics in quantum optics and solid-state physics under equilibrium conditions.^{1,2} The technique utilizes ever present spin fluctuations to measure the dynamics of spin ensembles via off-resonant optical Faraday rotation without disturbing the system. The technique is easy to use in atomic gases where the spin noise usually is of comparable size as optical shot noise.³ The large spin noise signal in atomic gases results from the long spin relaxation times and the sharp optical resonances. In semiconductors, typical spin relaxation times are much shorter and the optical resonances are significantly broader resulting in a spin noise signal which is usually orders of magnitude lower than the optical shot noise. As a consequence, SNS in semiconductors had not been demonstrated before 2005⁴ – more than 20 years after its first implementation in atom optics.¹ Nevertheless, already this first spin noise measurement on semiconductors indicated the huge advantage of SNS compared to the traditional optical probes which inherently disturb the system.

The first SNS experiment on semiconductors was carried out with an electrical sweeping spectrum analyzer resulting in a poor signal-to-noise ratio despite long integration times. This changed in 2007 by the introduction of real-time fast Fourier transformation (FFT) spectrum analyzers into SNS which optimized the data averaging and triggered the current success of SNS.⁵ Real-time FFT analyzers are by orders of magnitude more efficient than sweeping spectrum analyzers since they allow simultaneous detection of spin noise at all frequencies within the detection bandwidth and thus average over 100% of the measured data stream.⁶ Nowadays, SNS employing real-time FFT is routinely used to study the spin dynamics in many bulk and low dimensional semiconductors.^{7–12} However, the technique is limited to long spin dephasing times by the bandwidth of the detection system and in particular by the bandwidth of the electrical analog-to-digital (A/D) conversion via a digitizer. Up to now, most SNS experiments have been carried out on systems with

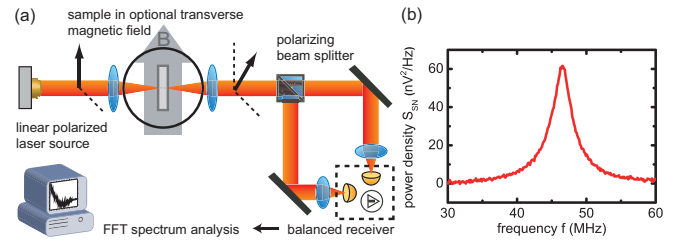


FIG. 1. (Color online) (a) Standard setup for semiconductor SNS. (b) Typical experimental spin noise power spectrum. The laser shot noise background is subtracted.

spin dephasing rates below 100 MHz which can be accurately resolved by fast 16-bit digitizers.^{5,7,8,10,12} Crooker *et al.* recently measured spin dephasing rates of a few 100 MHz by means of a 1-GHz digitizer card with a lower effective resolution (≈ 6 bit).¹¹ A universal application of semiconductor SNS, being relevant for technological application of SNS⁸ as well as for fundamental research,² certainly demands an extension of the available bandwidth exceeding 1 GHz by at least one order of magnitude. Ultrafast digitizers with a corresponding bandwidth of up to 13 GHz are commercially available, but show an effective resolution as low as 4 bit at their maximum frequency.

In this letter, we simulate realistic spin noise measurements to investigate to which extent the low bit depth of fast digitizers reduces the experimental sensitivity of SNS. As introduction, we first elucidate the typical experimental SNS setup, spin noise spectrum, spin noise power, and background shot noise level. Figure 1 (a) depicts the experimental SNS setup: Linear polarized probe light is transmitted through the sample and the acquired stochastic Faraday rotation is measured by means of a polarizing beam splitter and a balanced photo receiver. The time signal of the detector is seamlessly digitized, divided into blocks with fixed size of a power of two, and Fourier transformed. The resulting Fourier power spectra are added up for averaging. Figure 1 (b) depicts a showcase experimental spin noise spectrum $S_{SN}(f)$ [V^2/Hz] measured in *n*-doped bulk GaAs at cryogenic temperatures. The Lorentzian line shape results from a mono-

^{a)} Electronic mail: mueller@nano.uni-hannover.de

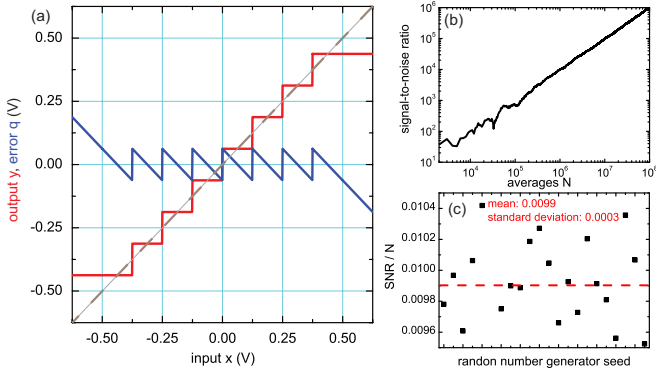


FIG. 2. (Color online) (a) Input-output characteristics of a symmetric midrise digitizer ($R = 3$ bit). (b) Signal-to-noise ratio (SNR) of an exemplary simulated spin noise measurement with N averages. (c) SNR/ N for different random number sets; all other data in this letter is acquired by means of the same set of random numbers.

exponential spin decay and is centered at the electron Larmor frequency f_L of the precessing spins with a full width at half maximum proportional to the spin dephasing rate $\Gamma = \pi w_{\text{FWHM}}$. The height of the spin noise peak $S_{\text{SN}}(f_L) = 2P_{\text{SN}}\Gamma^{-1}(\nu P_{\text{laser}})^2 [\text{V}^2/\text{Hz}]$ is determined by Γ and the Faraday rotation noise power $P_{\text{SN}} [\text{rad}^2]$, which in turn is given by the number and statistics of the probed spins and the detuning from the optical resonance.² The probe laser power is denoted by P_{laser} and the conversion gain of the detector by $\nu [\text{V}/\text{W}]$. Optical shot noise strongly contributes to the total observed noise signal as a white background noise with a power level $S_{\text{WN}} = 2\nu^2 \hbar \omega_{\text{laser}} P_{\text{laser}} [\text{V}^2/\text{Hz}]$.¹³ The low optical density as well as the high spin dephasing rates in semiconductors result in a very low ratio of peak spin noise density $S_{\text{SN}}(f_L)$ to the white background noise level S_{WN} : $\eta = P_{\text{SN}}\Gamma^{-1} \times P_{\text{laser}}/\hbar \omega_{\text{laser}}$. For typical semiconductor systems, η usually ranges from 10^{-2} to 10^{-4} and will be even smaller for prospective room temperature SNS measurements in n -type bulk GaAs ($\Gamma \gg 1 \text{ GHz}$)¹⁴ or for SNS of a single electron spin in an optical cavity, where P_{laser} is as low as $10 \mu\text{W}$ at the balanced receiver.^{15,16}

Next, we simulate such SNS measurements for the case of low signal strength η and fast digitizers with low resolution. The key figures of merit of a digitizer are the bit depth R and the sampling rate f_S .¹⁷ The sampling rate limits the bandwidth to $B = f_S/2$ according to the Nyquist-Shannon theorem.^{18,19} The bit depth defines the resolution of a digitizer. Figure 2(a) depicts the input-output characteristics of a uniform and symmetric midrise quantizer that is commonly employed in fast A/D converters. The digital output y of these digitizers deviates from the analog input signal x by a quantization error $q = y - x$ which results from the granularity and from the overload for $|x| > x_{\text{max}}$. We set $x_{\text{max}} = 0.5 \text{ V}$ throughout this letter. As long as q can be viewed as distributed independently of x , the granularity results in a

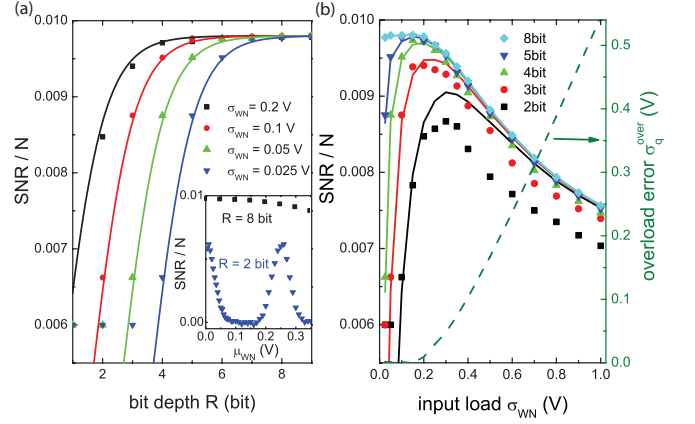


FIG. 3. (Color online) (a) SNR/ N ($N = 10^8$) as a function of bit depth for different voltage loads. The ratio of spin noise to shot noise is fixed to $\eta = 256 \times \alpha^2/\sigma_{\text{WN}}^2 = 0.01$. The solid lines are calculated by Eqs. (1) and (2) and corrected for the statistic deviation from 0.01. The inset shows SNR/ N as a function of a superimposed DC signal μ_{WN} revealing the effective 1-bit quantization at low input load. (b) SNR/ N ($N = 10^8$, $\eta = 256 \times \alpha^2/\sigma_{\text{WN}}^2 = 0.01$) as a function of input load for different bit depths. The broken line gives the overload error and is extracted from the difference between the curve in (a) and the values from the simulations for 8 bit. The solid lines are calculated with these values for $\sigma_{q, \text{over}}$ in Eq. (2).

standard deviation of q given by Bennett's formula where it is assumed that q is uniformly distributed and is limited to $-2^{-R}/2 < q < 2^{-R}/2$, i.e., no overload occurs:²⁰

$$\sigma_{q, \text{gran}} = 2^{-R}/\sqrt{12} \text{ V}. \quad (1)$$

In the following simulation of the spin noise measurements, we systematically vary the bit depth of the digitizer and the voltage load at the digitizer input in order to study the influence of the A/D conversion on the experimental sensitivity of SNS. The input consists of $N \times 1024$ samples. The spin noise is represented by a sine waveform with amplitude $\alpha [\text{V}]$ and a fixed frequency $f_L = f_S/8$ which is added to random number generated white Gaussian background noise with zero mean and the standard deviation $\sigma_{\text{WN}} [\text{V}]$.²¹ The digital data is produced by a simulated R -bit digitizer corresponding to Fig. 2 (a) and blocks of 1024 points are Fourier transformed via the FFT algorithm. The resulting power spectra are averaged and yield the spin noise spectrum $S(f) [\text{V}^2/\text{Hz}]$. The spin noise signal strength is measured by the signal-to-noise ratio (SNR) which is extracted from the simulations as $\text{SNR} = [S(f_L) - \mu_S]/\sigma_S$, where μ_S and σ_S denote the mean and standard deviation of $S(f)$ with $0 < f \leq B$, $f \neq f_L$, respectively. All spin noise power is detected in a single frequency bin f_L and the magnitude of the spin noise peak is given by $S_{\text{SN}}(f_L) = \alpha^2/2 \times 512/B$ on top of the shot noise floor of $S_{\text{WN}} = \sigma_{\text{WN}}^2/B$. All simulation data that is shown in this letter is acquired with fixed relative signal strength

$\eta = S_{\text{SN}}(f_L)/S_{\text{WN}} = 256 \times \alpha^2/\sigma_{\text{WN}}^2 = 0.01$ since the following conclusions are independent of η for $\eta \ll 1$. Keeping η fix while varying σ_{WN} corresponds to simultaneous amplification of spin noise and background noise by a voltage amplifier in the experiment.

Figure 2 (b) exemplarily shows the signal-to-noise ratio as a function of the averages N for a certain set of simulation parameters. The signal-to-noise ratio increases linearly with N and the slope SNR/N directly gives a measure for the detection sensitivity. Figure 2 (c) shows SNR/N for several simulations with the same parameter set but with different seeds for the pseudo random number generator. The theoretically expected mean value of 0.01, which is derived below, is well within the error interval around the mean of $\mu_{\text{SNR}/N} = 0.0099(3)$. In order to cope with the long computing times, we waive statistic averaging of the simulation results in the following and carry out all simulation runs with the same set of random numbers to ensure comparability between different parameters.

Figure 3 (a) shows SNR/N as a function of the bit depth R for 10^8 averages and different σ_{WN} . The simulations reveal for an optimal input load of $\sigma_{\text{WN}} = 0.1\dots 0.2$ V a significant decrease of the detection sensitivity only for $R \leq 3$ bit.²² Lower than optimal input voltages effectively reduce the bit depth and the granular quantization error becomes significant also for digitizers with a nominally higher bit depth. Given Eq. (1), the rather weak influence of the bit depth in Fig. 3 (a) may at first seem surprising. However, the white shot noise can be viewed as additive dither to the spin noise signal which helps to detect spin noise with an amplitude much smaller than the size of the least significant bit 2^{-R} V. The implications of such additive dither on quantization have already been subject of several investigations in information theory^{23–26} and were also considered in connection with data averaging.^{27–31} However, especially the overload errors, which can be important in SNS, have been greatly neglected so far. We want to point out that purposely adding noise in digital data averaging can under certain circumstances reduce the quantization error, however, the white shot noise in semiconductor SNS is much higher than the optimal amount of dither,³¹ i.e., optical shot noise is not a remedy but an obstacle in SNS.

Next, we discuss the granular and the overload error in more detail. The standard deviation of the spin noise spectrum S is composed of contributions from the white optical shot noise σ_{WN} , the granular quantization noise $\sigma_{q, \text{gran}}$, and the overload noise $\sigma_{q, \text{over}}$:

$$\sigma_S = \frac{1}{B} \sqrt{\sigma_{\text{WN}}^2 + \sigma_{q, \text{gran}}^2 + \sigma_{q, \text{over}}^2} \left[\frac{\text{V}^2}{\text{Hz}} \right]. \quad (2)$$

The signal-to-noise ratio extracted from the simulations reads accordingly $\text{SNR} = 256 \alpha^2/(B\sigma_S^2) \times N$. First, we point out that the linear increase of signal-to-noise ratio with N is found in the simulations for all tested parameter sets. Deviation from this linear behavior as reported in Ref. 31 is not expected due to the larger amount of

dither present in our simulations. We further confirmed the proportionality between the signal-to-noise ratio and α^2 in the simulations over four orders of magnitude from $\eta = 10^{-1}$ to $\eta = 10^{-4}$. The granular quantization error at lower bit depths is well modeled by Eq. (1) (solid lines in Fig. 3 (a)). However, a significantly smaller quantization error in the simulations than in Bennett’s formula is found at $R = 1$ bit or at effective 1-bit quantization in the case of low input load. This observation is not surprising since the assumption for Eq. (1) that the quantization error is independent of the input obviously collapses for 1-bit quantization.³² We note that low input load at low bit rates results in effective 1-bit quantization, which theoretically shows a decent detection sensitivity. However, this theoretical sensitivity is not of experimental relevance since even the smallest DC offset μ_{WN} yields a drastic drop of the signal-to-noise ratio as visualized in the inset of Fig. 3 (a). On the other hand, input overload, which becomes significant above $\sigma_{\text{WN}} = 0.2\dots 0.3$ V, equally destroys the efficiency of the spin noise detection even at high bit depth. Figure 3 (b) depicts SNR/N as a function of σ_{WN} for different R . The overload error for 8 bit (broken line) is extracted from the simulation results in conjunction with Eqs. (1) and (2) and is in turn utilized for calculating SNR/N for the different bit depths (solid lines), revealing that the overload error slightly depends on R . The optimal voltage load, which is found to be independent of spin noise power, varies from $\sigma_{\text{WN}} \approx 0.1$ V (8 bit) to $\sigma_{\text{WN}} \approx 0.3$ V (2 bit). Interestingly, these values coincide with the literature values for optimal load in the case of a normally distributed signal in the absence of dither.^{17,33}

In conclusion, we simulated spin noise measurements with FFT real-time data acquisition by means of a digitizer with low resolution and determined the optimal input load at the digitizer for efficient data averaging. The simulations prove that, at well chosen input load, fast A/D converters with few effective bits allow SNS with excellent sensitivity. The simulations pave the way towards high bandwidth SNS with commercial ultrafast digitizers exceeding frequencies of 10 GHz. The experimental bandwidth that is accordingly accessible with current technology is more than one order of magnitude larger than the highest currently demonstrated bandwidth.³⁴ Such an increase in bandwidth erases one of the main obstacles of SNS and will allow, e.g., SNS on GaAs at room temperature and, consequently, spatially resolved three-dimensional, non-destructive doping concentration measurements at room temperature.⁸ We want to point out, that the results of this letter apply in general to all similar experiments employing A/D conversion where a small signal with high bandwidth is detected in the presence of strong background noise.

The authors thank S.A. Crooker for helpful discussions. This work was supported by the German Science Foundation (DFG priority program 1285 ‘Semiconductor Spintronics’), the Federal Ministry for Education and Research (BMBF NanoQUIT), and the Centre for Quan-

tum Engineering and Space-Time Research in Hannover (QUEST). G.M.M. acknowledges support from the Evangelisches Studienwerk.

- ¹E. B. Aleksandrov and V. S. Zapasskii, Sov. Phys. JETP **54**, 64 (1981).
- ²G. M. Müller, M. Oestreich, M. Römer, and J. Hübner, Physica E, doi:10.1016/j.physe.2010.08.010 (2010).
- ³S. A. Crooker, D. G. Rickel, A. V. Balatsky and D. L. Smith, Nature **431**, 49 (2004).
- ⁴M. Oestreich, M. Römer, R. J. Haug, and D. Hägele, Phys. Rev. Lett. **95**, 216603 (2005).
- ⁵M. Römer, J. Hübner, and M. Oestreich, Rev. Sci. Instrum. **78**, 103903 (2007).
- ⁶A sweeping spectrum analyzer that was used in Ref. 4, e.g., with a bandwidth of 100 MHz and a resolution bandwidth of 0.1 MHz exploits only $\sim 0.1\%$ of the relevant information carried in the signal.
- ⁷G. M. Müller, M. Römer, D. Schuh, W. Wegscheider, J. Hübner, and M. Oestreich, Phys. Rev. Lett. **101**, 206601 (2008).
- ⁸M. Römer, J. Hübner, and M. Oestreich, Appl. Phys. Lett. **94**, 112105 (2009).
- ⁹S. A. Crooker, L. Cheng, and D. L. Smith, Phys. Rev. B **79**, 035208 (2009).
- ¹⁰M. Römer, H. Bernien, G. Müller, D. Schuh, J. Hübner, and M. Oestreich, Phys. Rev. B **81**, 075216 (2010).
- ¹¹S. A. Crooker, J. Brandt, C. Sandfort, A. Greilich, D. R. Yakovlev, D. Reuter, A. D. Wieck, and M. Bayer, Phys. Rev. Lett. **104**, 036601 (2010).
- ¹²G. M. Müller, M. Römer, J. Hübner, and M. Oestreich, Phys. Rev. B **81**, 121202(R) (2010).
- ¹³Electrical detector noise further contributes to the noise background, but only becomes significant at low probe laser power.
- ¹⁴S. Oertel, J. Hübner, and M. Oestreich, Appl. Phys. Lett. **93**, 132112 (2008).
- ¹⁵J. Berezovsky, M. H. Mikkelsen, O. Gywat, N. G. Stoltz, L. A. Coldren, and D. D. Awschalom, Science **314**, 1916 (2006).
- ¹⁶See also Tab. 1 of Ref. 2.
- ¹⁷N. S. Jayant and P. Noll, *Digital Coding of Waveforms: Principles and Applications to Speech and Video* (Prentice Hall, Englewood Cliffs 1984), first printing edition.
- ¹⁸H. Nyquist, Trans. AIEE **47**, 617 (1928).
- ¹⁹C. E. Shannon, Proc. IRE **37**, 10 (1949).
- ²⁰W. R. Bennett, Bell Syst. Tech. J. **27**, 446 (1948).
- ²¹It is carefully assured that the output of the used pseudo random number generator shows no correlations that reduce the efficiency of the averaging process. The periodicity of the employed algorithm exceeds 10^{57} samples.
- ²²As $\eta \ll 1$, the input load is basically given by σ_{WN} .
- ²³L. Schuchman, IEEE Trans. Commun. **12**, 162 (1964).
- ²⁴J. Vanderkooy and S. Lipshitz, J. Audio Eng. Soc. **32**, 106 (1984).
- ²⁵R. Gray and J. Stockham, T.G., IEEE Trans. Inf. Theory **39**, 805 (1993).
- ²⁶R. Wannamaker, S. Lipshitz, J. Vanderkooy, and J. Wright, IEEE Trans. Signal Process. **48**, 499 (2000).
- ²⁷R. Belchamber and G. Horlick, Talanta **28**, 547 (1981).
- ²⁸P. Carbone and D. Petri, IEEE Trans. Instrum. Meas. **43**, 389 (1994).
- ²⁹P. Carbone and D. Petri, IEEE Trans. Instrum. Meas. **49**, 337 (2000).
- ³⁰P. J. B. Koeck, Signal Process. **81**, 345 (2001).
- ³¹R. Skartlien and L. Oyeaug, IEEE Trans. Instrum. Meas. **54**, 1303 (2005).
- ³²R. Gray, IEEE Trans. Inf. Theory **36**, 1220 (1990).
- ³³J. Max, IRE Trans. Inf. Theory **6**, 7 (1960).
- ³⁴For ultrahigh frequencies, the balanced receiver can be substituted by a single, ultrafast photodiode, if the classical laser noise is suppressed, e.g., by interferometry.